

Phase separation in strained epitaxial InGaN islands

Xiaobin Niu, Gerald B. Stringfellow, and Feng Liu

Citation: *Appl. Phys. Lett.* **99**, 213102 (2011); doi: 10.1063/1.3662927

View online: <http://dx.doi.org/10.1063/1.3662927>

View Table of Contents: <http://apl.aip.org/resource/1/APPLAB/v99/i21>

Published by the [American Institute of Physics](#).

Related Articles

Equilibrium compositional distribution in freestanding ternary semiconductor quantum dots: The case of $\text{In}_x\text{Ga}_{1-x}\text{As}$

J. Chem. Phys. **135**, 234701 (2011)

Phase separation and exchange biasing in the ferromagnetic IV-VI semiconductor $\text{Ge}_{1-x}\text{Mn}_x\text{Te}$

Appl. Phys. Lett. **97**, 023101 (2010)

Evolution of phase separation in In-rich InGaN alloys

Appl. Phys. Lett. **96**, 232105 (2010)

MnSe phase segregation during heteroepitaxy of Mn doped Ga_2Se_3 on Si(001)

Appl. Phys. Lett. **95**, 241907 (2009)

Thermal anomalies in ternary $\text{Ge}_{42-x}\text{Pb}_x\text{Se}_{58}$ glasses near the charge carrier reversal threshold

J. Appl. Phys. **106**, 113516 (2009)

Additional information on *Appl. Phys. Lett.*

Journal Homepage: <http://apl.aip.org/>

Journal Information: http://apl.aip.org/about/about_the_journal

Top downloads: http://apl.aip.org/features/most_downloaded

Information for Authors: <http://apl.aip.org/authors>

ADVERTISEMENT



HAVE YOU HEARD?

Employers hiring scientists
and engineers trust
physicstodayJOBS



<http://careers.physicstoday.org/post.cfm>

Phase separation in strained epitaxial InGaN islands

Xiaobin Niu,¹ Gerald B. Stringfellow,^{1,2} and Feng Liu^{1,a)}

¹Department of Materials Science and Engineering, University of Utah, Salt Lake City, Utah 84112, USA

²Department of Electrical and Computer Engineering, University of Utah, Salt Lake City, Utah 84112, USA

(Received 21 September 2011; accepted 29 October 2011; published online 21 November 2011)

Phase separation (PS) produces InN composition gradients in InGaN islands, which may be important for light emitting diodes, solar cells, and lasers. Thus, the control of PS is critical, and the kinetic growth process, which is suggested to be important for controlling PS in Stranski-Krastanov islands, becomes a key factor in producing materials for optoelectronic devices. We present atomistic-strain-model Monte Carlo simulations for PS in strained epitaxial InGaN islands. Our simulations illustrate how the PS in InGaN islands depends on the kinetic growth mode and subsurface diffusion, and thus suggest ideas for controlling the microstructure of alloy islands formed during epitaxial growth. © 2011 American Institute of Physics. [doi:10.1063/1.3662927]

The bandgap of InGaN can be tuned from 0.7 to 3.4 eV, covering the entire spectrum from UV to IR. Because of the wide range of bandgap tunability in this single alloy system, it is currently being investigated for optoelectronic devices, such as high efficiency blue, green, and white light emitting diodes (LEDs),¹ solar cells,² and injection lasers.³ It has been reported that phase separation (PS) improves the performance of LEDs and lasers.⁴ Thus, PS in InGaN alloy islands to produce InN composition gradients becomes a key factor in producing materials for LEDs and lasers.

The tendency of bulk InGaN alloy to PS due to the miscibility gap has been known for more than a decade.^{4,5} In epitaxial systems, the immiscibility of InGaN is strongly dependent on elastic strain due to lattice mismatch between the InGaN and the substrate. Since the early study of Ho and Stringfellow,⁵ work has been done to study PS in epitaxial InGaN layers both theoretically and experimentally.⁶⁻⁹ InGaN layers coherently grown on GaN are under compressive strain. This compressive strain tends to suppress PS of InGaN layers at typical growth temperatures.⁸ The theoretical studies to date, in particular, first-principles and valence force field calculations, are limited to the determination of the bonding energy terms in bulk InGaN alloys (either strained or relaxed).^{8,9} However, these bulk parameters cannot be used to study growth of Stranski-Krastanov (S-K) islands. This is because strain relaxation and surface effects, which cannot be accounted for by bulk parameters, significantly affect the spatial variation of InN content in S-K islands. This prevents us from reaching a complete and correct understanding of PS in the strained S-K InGaN islands. To our best knowledge, there is no published work on PS in strained S-K InGaN islands.

It is anticipated that particular kinetic aspects of the growth process will be important for controlling PS in S-K islands.¹⁰ Control of the PS in the strained epitaxial InGaN islands can be achieved only by having a clear picture of the physical growth mechanism. The entire S-K islands are not expected to reach thermodynamic equilibrium because bulk diffusion is negligible at typical growth temperatures.¹¹

Growth usually occurs under non-equilibrium conditions. However, equilibrium is often established locally at the growth front (near surface region) due to the more rapid surface (and sub-surface) diffusion.¹² Thus, distinctly different InN distributions from equilibrium would be obtained. This has been predicted by our recent work on GeSi islands.¹⁰ The objective of this letter is to examine the effects of the kinetic growth mode and subsurface diffusion on PS in strained epitaxial InGaN islands, and the use of this understanding to provide guidance for control of the microstructure of the InGaN alloys formed during epitaxial growth.

To study kinetically controlled PS in epitaxial strained InGaN islands and its underlying relationship to the kinetic growth mode, subsurface diffusion, and strain from the substrate, we have performed atomistic-strain-model Monte Carlo simulations^{10,13} of the epitaxial growth of strained InGaN islands by considering two different growth modes: layer-by-layer growth (LG) versus faceted growth (FG). Experiments¹⁴ showed that some islands grow first layer-by-layer in a non-faceted structure like stepped mounds and then transform into the faceted structures after the mounds reach a certain size. Therefore, it is reasonable to consider both growth modes because even the final island is faceted its alloy composition is influenced by its early stage growth in the LG mode. Our calculations show that for GaN substrates, LG produces islands that are InN rich on the top and sides (shell); while FG produces islands that are InN rich in the middle (core). The composition profiles in S-K islands with growth-mode-controlled PS are shown to be distinctly different from the equilibrium results.^{10,15}

PS during the epitaxial growth of InGaN islands is simulated by minimizing the Gibbs free energy, $G = H - TS$. The enthalpy $H = E_{el} + E_s$, where the total elastic strain energy E_{el} is calculated using an atomistic strain model¹⁶ and includes the micro-strain energy due to the bond distortion in the islands and the macro-strain energy associated with the lattice mismatch between the islands and the substrate. E_s is the surface energy, which is considered here as the bond-breaking energy at the surface without reconstruction. The entropy of mixing, S , is calculated using the regular-solution-shell-model.¹⁰ Using the experimental elastic constants of $\text{In}_x\text{Ga}_{1-x}\text{N}$, our model produces the interaction parameter for mixing,

^{a)} Author to whom correspondence should be addressed. Electronic mail: fliu@eng.utah.edu.

$\Omega_{\text{InGaN}} = -5.16 \times 10^{-4}x + 0.36 \text{ eV/cation}$, which agrees well with previous first principles¹⁷ and valence force field results.¹⁸ Since three-dimensional (3D) simulations were found to show qualitatively similar results as 2D simulations,¹⁰ we have used mainly a 2D atomistic strain model on a square lattice to calculate the Gibbs free energy. The detailed simulation framework is described in our previous work.¹⁰

First, we studied the growth mode controlled PS that leads to a core-shell nanostructure in $\text{In}_{0.3}\text{Ga}_{0.7}\text{N}$ islands grown on GaN. The thermodynamic equilibrium distribution is generally not expected for larger nanostructures although it may be reached in small structures grown at high temperatures, where diffusion allows redistribution of the alloy components within the entire structures. This is because the bulk diffusion barrier is too high, e.g., $\sim 3.4 \text{ eV}$, at typical growth temperatures for diffusion of In and Ga in InGaN.¹¹ However, local equilibrium can be established in the surface regions during the growth since the diffusion is greatly enhanced at surfaces. For example, diffusion activation energies of $\sim 0.4 \text{ eV}$ are reported for Ga surface diffusion on GaN(0001).¹² Consequently, the kinetic growth mode, which dictates the surface mass transport and alloy mixing via surface diffusion at the growth front, becomes a key factor in determining the kinetically limited composition profiles in S-K islands with PS.

Figs. 1(a) and 1(e) show a limiting case using the assumption that the surface diffusion depth (L_{SD}) is 1, which means that the local equilibrium is reached only in the outmost surface (or facet) layer and the equilibrated surface composition is subsequently frozen upon the growth of the following layer. It is seen that such kinetically limited PS during growth leads to the formation of core-shell structured islands. The LG yields structures with cores rich in the unstrained (relative to the substrate) component (Fig. 1(a), $x_{\text{Ga}} > 0.8$ in the core); while the FG yields structures with cores rich in the strained (relative to the substrate) component (Fig. 1(e), $x_{\text{In}} > 0.8$ in the core). Both growth modes result in structures distinctly different from the equilibrium case.¹⁵ These results are due to the different strain relaxation mechanisms associated with the two different growth modes. In the LG mode, the growth front is flat and the most relaxed regions are at the opposite sides. During establishment of the local equilibrium within this flat layer, a “lateral” PS with the In segregating to the outside and Ga to the center of the surface layer is expected to reduce the strain energy. In contrast, in the FG mode, the growth front is inclined at a fixed contact angle with the nominal substrate surface and the strain is relaxed most at the top of the facet, furthest from the substrate. During the establishment of local equilibrium within this inclined facet layer, a “vertical” PS with In segregating to the top and Ga to the bottom of the facet is favored. Such lateral versus vertical PS patterns in the LG versus FG gives rise to the overall core-shell structures of InGaN islands.

There is another notable difference between core-shell structures resulting from the two growth modes. A triangle core shape is found in LG, and a V-shape core in FG. This is because as the island grows larger in the LG mode, fewer In atoms are segregated to the outside since the growth front becomes smaller, assuming a fixed nominal alloy concentration is deposited in each layer. This leads to the triangular shaped core seen in Fig. 1(a). On the contrary, more In atoms

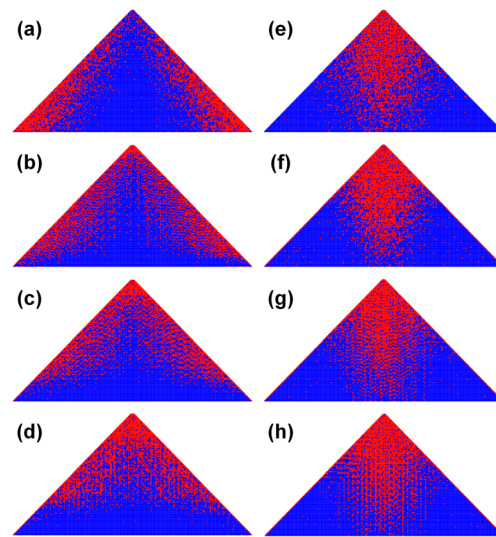


FIG. 1. (Color online) Kinetically controlled atomistic distribution (InN-red, GaN-blue) for heteroepitaxial $\text{In}_{0.3}\text{Ga}_{0.7}\text{N}$ QDs grown on GaN substrates when local equilibration is assumed for several surface layers at the growth front. The left panel shows the triangle-shaped GaN-rich core distributions resulting from the LG mode, and the right panel shows the V-shaped InN-rich core distributions resulting from the FG mode. Equilibration is assumed in the top (a) and (e) 1, (b) and (f) 4, (c) and (g) 7, (d) and (h) 10 surface layers.

are segregated to the top as the island grows larger in the FG mode since the growth front becomes larger. This leads to the V-shaped core seen in Fig. 1(e). This V-shaped core structure seen in Fig. 1(e) is consistent with experimental results as well as a qualitative theoretical explanation for $\text{In}_{0.5}\text{Ga}_{0.5}\text{As}$ islands grown on GaAs substrates,¹⁹ indicating that the InGaAs islands were grown via the FG mode. Note here we compare our result with InGaAs because no experimental data for InGaN islands have been reported.

The restriction of limiting the local equilibration within the surface layer ($L_{SD} = 1$) might be too severe. The region of enhanced diffusion and local equilibration may extend to several subsurface layers.²⁰ Thus, we have studied the effects of L_{SD} on the PS in the islands. Figs. 1(c)–1(h) show the simulated InN atomistic distribution of a strained $\text{In}_{0.3}\text{Ga}_{0.7}\text{N}$ island grown by the LG mode (Figs. 1(b)–1(d)) versus the FG mode (Figs. 1(f)–1(h)) with L_{SD} values of 4 (Figs. 1(b) and 1(f)), 7 (Figs. 1(c) and 1(g)), and 10 (Figs. 1(d) and 1(h)), respectively. These results clearly show the impact of diffusion depth on the final structure. As expected, increasing the L_{SD} causes the core-shell structure to gradually disappear and the final structure obtained from both growth modes to converge towards the equilibrium structure.¹⁵

Surface segregation affects PS of InGaN islands in both growth modes. Because the surface energy of In is lower than for Ga, which is caused by both the surface dangling bond energy and strain energy, In tends to occupy the outmost surface layer during the growth process. Fig. 2 shows the time evolution of the atomistic view of InN distribution for $\text{In}_{0.3}\text{Ga}_{0.7}\text{N}$ islands in Figs. 1(c) (top panel) and 1(g) (bottom panel), illustrating the effect of InN surface segregation. Notice that the island surface layer is covered by a complete monolayer of InN at all stages in both growth modes.

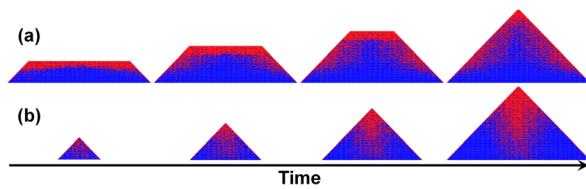


FIG. 2. (Color online) Non-equilibrium atomistic distribution (InN-red, GaN-blue) for heteroepitaxial $\text{In}_{0.3}\text{Ga}_{0.7}\text{N}$ QDs grown by (a) LG and (b) FG on GaN substrates, when local equilibration is assumed for 7 surface layers at the growth front. From left to right, the figure shows QDs when the growth is stopped after 30, 50, 70, and 100 monolayers. During the growth of QDs, the surface is fully covered by a monolayer of InN.

As described above, control of PS can be theoretically achieved by altering the growth mode. The growth mode is generally determined by growth parameters and/or by surface conditions.²¹ However, selecting the growth mode is complex. An alternative way to control the PS is to control the magnitude and sign of the strain in the islands by choice of substrate since the “unstrained component” is determined by the substrate. Thus, we have studied the influence of the substrate with different alloy compositions. The top panel of Fig. 3 shows the calculated atomistic InN distribution of $\text{In}_{0.7}\text{Ga}_{0.3}\text{N}$ islands grown by the LG mode (Fig. 3(a)) versus the FG mode (Fig. 3(b)) on an InN substrate, with $L_{SD}^* = 1$. Compared with the results shown in Figs. 1(a) and 1(e), this clearly shows the impact of a different substrate on the PS. The final phase separated islands switch their components in the core and shell in both growth modes since the “unstrained component” changes from GaN to InN as the substrate changes from GaN to InN.

In all of the results presented above, the macro-strain between the island and substrate plays an essential role. Next, we will examine the situation without macro-strain, i.e., the islands and the substrate are lattice matched or more simply have the same alloy composition. Because there is no macro-strain applied to the InGaN islands, they will phase separate into two domains due to the miscibility gap. The PS will lower the energy of the alloy system at the cost of increasing the interface energy between the two domains and the macro-strain energy between island and substrate. The final structure is determined by the competition between these factors. Our study shows that the lattice matched substrate will suppress PS in islands, and there exists a critical value of L_{SD}^* . Below L_{SD}^* , a uniform distribution of the components is expected throughout the island; above L_{SD}^* , the alloy will phase separate into In-rich and Ga-rich domains, with the smallest possible interface area between them. The atomistic InN distributions of $\text{In}_{0.5}\text{Ga}_{0.5}\text{N}$ islands grown by the LG mode (Fig. 3(c)) versus the FG mode (Fig. 3(d)) on the $\text{In}_{0.5}\text{Ga}_{0.5}\text{N}$ substrate with L_{SD}^* are shown in Fig. 3, bottom panel. One should also notice that L_{SD}^* is much larger for LG than for FG. This is because for LG, the island has a much larger interface with the substrate.

In summary, composition profiles in S-K islands with PS can be controlled by altering the growth mode (LG versus FG). Different substrates introduce different strain magnitude, and sign, which affects the final structures of the island. For islands grown on a lattice matched substrate, which will suppress the PS, PS will only happen when L_{SD} is larger than the

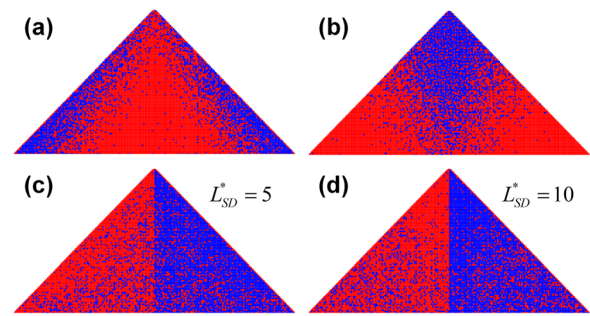


FIG. 3. (Color online) The influence of the substrate for two alloy compositions. Top panel shows the calculated atomistic distribution (InN-red, GaN-blue) for $\text{In}_{0.7}\text{Ga}_{0.3}\text{N}$ islands grown by (a) the LG mode versus (b) the FG mode on InN substrates, with $L_{SD}^* = 1$. It shows the reverse atom distributions compared with those grown on GaN (Figs. 1(a) and 1(e)). The bottom panel shows the atomistic distributions for $\text{In}_{0.5}\text{Ga}_{0.5}\text{N}$ islands grown by (c) the LG mode with $L_{SD}^* = 5$ versus (d) the FG mode with $L_{SD}^* = 10$ on $\text{In}_{0.5}\text{Ga}_{0.5}\text{N}$ substrates.

critical value L_{SD}^* . Our findings form a fundamental basis for developing useful technologies and point to a practical way to tailor and control the PS in the InGaN islands by selecting the growth mode and substrate. Such technology would be generally applicable to the development of strained alloy nanostructures for applications in photonic and electronic devices.

This work was supported financially by the DOE-BES division (Grant No. DE-FG02-04ER46148) and the Cao Group. We acknowledge NERSC and the CHPC at University of Utah for providing the computing resources.

¹S. Nakamura and G. Fasol, *The Blue Laser Diode: GaN Based Light Emitters and Lasers* (Springer, Berlin, 1997).

²O. Jani, I. Ferguson, C. Honsberg, and S. Kurtz, *Appl. Phys. Lett.* **91**, 132117 (2007).

³H. J. Choi, J. C. Johnson, R. He, S.-K. Lee, F. Kim, P. Pauzauskie, J. Goldberger, R. J. Saykally, and P. Yang, *J. Phys. Chem. B* **107**, 8721 (2003).

⁴Y. S. Lin, K. J. Ma, C. Hsu, S. W. Feng, Y. C. Cheng, C. C. Liao, C. C. Yang, C. C. Chou, C. M. Lee, and J. I. Chyi, *Appl. Phys. Lett.* **77**, 2988 (2000).

⁵I. Ho and G. B. Stringfellow, *Appl. Phys. Lett.* **69**, 2701 (1996).

⁶N. Faleev, B. Jampana, O. Jani, H. Yu, R. Opila, I. Ferguson, and C. Honsberg, *Appl. Phys. Lett.* **95**, 051915 (2009).

⁷V. Potin, E. Hahn, A. Rosenauer, D. Gerthsen, B. Kuhn, F. Scholz, A. Dus-saigne, B. Damilano, and N. Grandjean, *J. Cryst. Growth* **262**, 145 (2004).

⁸S. Y. Karpov, N. I. Podolskaya, I. A. Zhmakin, and A. I. Zhmakin, *Phys. Rev. B* **70**, 235203 (2004).

⁹C. K. Gan, Y. P. Feng, and D. J. Srolovitz, *Phys. Rev. B* **73**, 235214 (2006).

¹⁰X. B. Niu, G. B. Stringfellow, and F. Liu, *Phys. Rev. Lett.* **107**, 076101 (2011).

¹¹C. C. Chuo, C. M. Lee, and J. I. Chyi, *Appl. Phys. Lett.* **78**, 314 (2001).

¹²T. K. Zywiets, J. Neugebauer, and M. Scheffler, *Appl. Phys. Lett.* **73**, 487 (1998).

¹³J. M. Reich, X. B. Niu, Y. J. Lee, R. E. Caffisch, and C. Ratsch, *Phys. Rev. B* **79**, 073405 (2009).

¹⁴P. Sutter and M. G. Lagally, *Phys. Rev. Lett.* **84**, 4637 (2000); R. M. Tromp, F. M. Ross, and M. C. Reuter, *Phys. Rev. Lett.* **84**, 4641 (2000).

¹⁵See supplementary material at <http://dx.doi.org/10.1063/1.3662927> for equilibrium results.

¹⁶A. C. Schindler, M. F. Gyure, G. D. Simms, D. D. Vvedensky, R. E. Caffisch, C. Connell, and E. Luo, *Phys. Rev. B* **67**, 075316 (2003).

¹⁷D. L. A. Camacho, R. H. Hopper, G. M. Lin, B. S. Myers, M. Van Schilfhaar, A. Sher, and A. B. Chen, *J. Cryst. Growth* **178**, 8 (1997).

¹⁸T. Saito and Y. Arakawa, *Phys. Rev. B* **60**, 1701 (1999).

¹⁹N. Liu, J. Tersoff, O. Baklenov, A. L. Holmes, Jr., and C. K. Shih, *Phys. Rev. Lett.* **84**, 334 (2000).

²⁰F. Liu and M. G. Lagally, *Phys. Rev. Lett.* **76**, 3156 (1996).

²¹J. Zhu, F. Liu, and G. B. Stringfellow, *Phys. Rev. Lett.* **101**, 196103 (2008).